

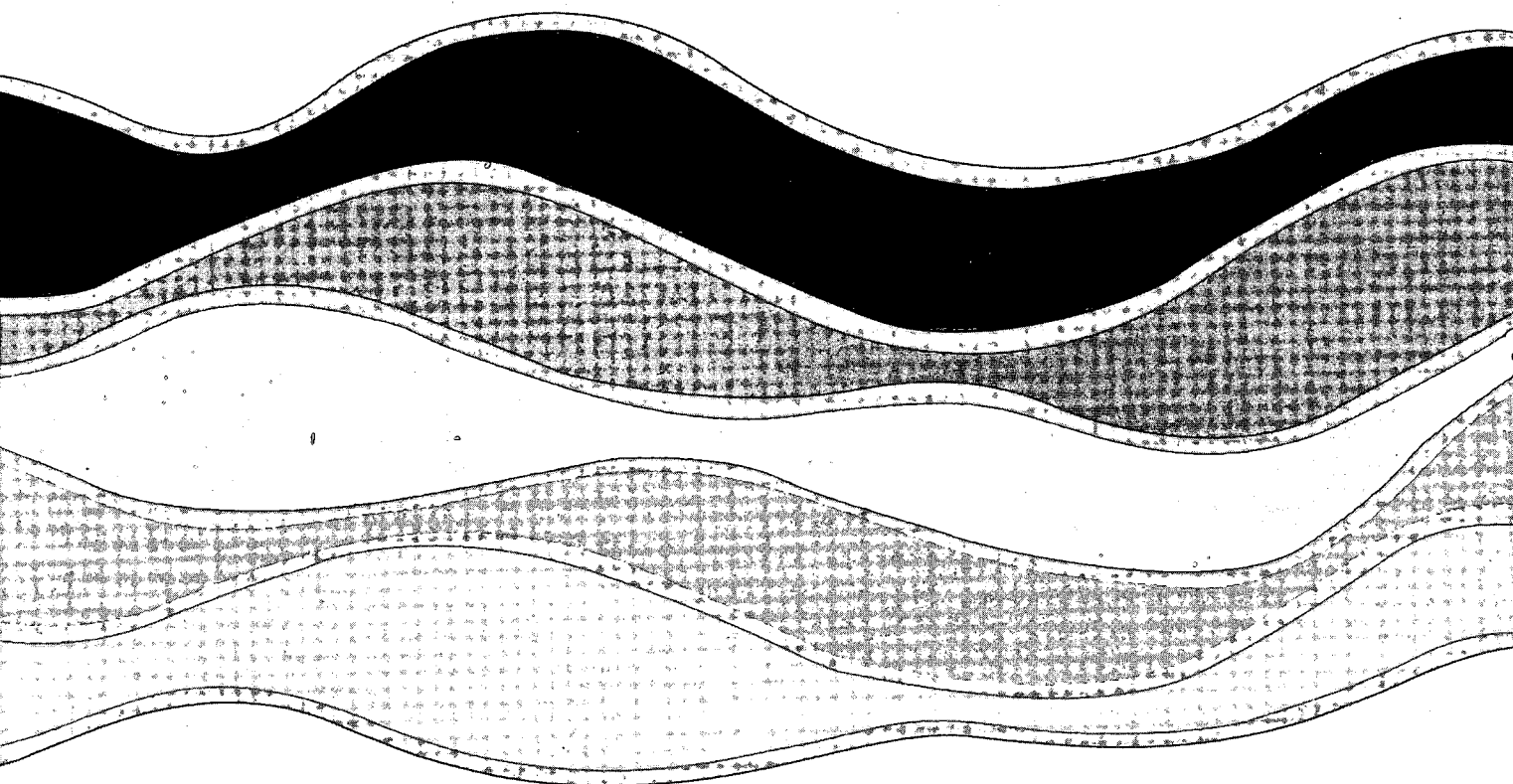
**CCIW**

NOV 14 1991

**LIBRARY**

**NATIONAL  
WATER  
RESEARCH  
INSTITUTE**

**INSTITUT  
NATIONAL  
de RECHERCHE  
sur les  
EAUX**



**EDDY CORRELATION MEASUREMENTS OF  
AIR-SEA FLUXES FOR A DISCUS BUOY**

**F. Ancil and M.A. Donelan**

**NWRI Contribution No. 91-121**

TD  
226  
N87  
No. 91-  
121  
c. 1

**Eddy Correlation Measurements of Air-Sea Fluxes**  
**from a Discus Buoy.**

by

**François Anctil**  
Université Laval, génie civil  
Québec, Québec, CANADA, G1K 7P4

and

**Mark A. Donelan**  
National Water Research Institute, Canada Centre for Inland Waters  
Burlington, Ontario, CANADA, L7R 4A6

to be submitted to  
**Journal of Atmospheric and Oceanic Technology**

June 1991

## MANAGEMENT PERSPECTIVE

The importance of a full understanding of the coupling between the atmosphere and oceans and lakes has been brought into sharp focus by the difficult demands of climatic change modelling. In large part, progress in understanding air-sea coupling mechanisms is retarded by the difficulty of obtaining suitable data in storm conditions far from land. Three meter (diameter) discus buoys are finding common use both as meteorological stations and as wave directional measuring platforms. They are relatively small and inexpensive (for ocean going buoys) and, with their existing wind and wave measurements, are ideally suited for exploring the air-sea coupling of momentum, heat and mass, since these are affected by both wave and wind. This paper demonstrates that with a modest amount of additional equipment these buoys can be made to measure the direct flux of momentum. The method is tested against measurements made during the Surface Wave Dynamics Experiment.

## **SOMMAIRE À L'INTENTION DE LA DIRECTION**

L'importance de bien comprendre le couplage entre l'atmosphère et les océans et les lacs a été mise bien en évidence par les exigences complexes de la modélisation du changement climatique. Dans une grande mesure, les progrès au niveau de la connaissance des mécanismes de couplage air-mer sont retardés en raison de la difficulté d'obtenir des données appropriées sur les conditions de tempête loin de la côte. Des bouées en forme de disque de trois mètres de diamètre sont utilisées couramment comme stations météorologiques et comme plate-formes de mesure de la direction des vagues. Elles sont relativement petites et peu coûteuses (pour des bouées utilisées en mer) et grâce à leurs dispositifs existants de mesure du vent et des vagues, elles conviennent très bien à l'étude du couplage air-mer du momentum, de la chaleur et de la masse, étant donné qu'elles subissent à la fois l'influence des vagues et du vent. Le présent article montre que ces bouées, accompagnées de peu d'autres appareils, peuvent mesurer le flux direct du momentum. La méthode est vérifiée en fonction de mesures effectuées au cours de l'expérience sur le terrain de l'évolution des vagues (SWADE).

## **Abstract**

This paper demonstrates that it is possible to measure turbulent air-sea fluxes from a discus buoy. It proposes a method to correct the measured wind flow, for velocities induced by angular and axial movements of the anemometer, allowing the estimation of the momentum, sensible heat and latent heat fluxes. A subset of the data gathered during the Surface Wave Dynamics Experiment (SWADE) is used to test the method. Successful evaluation of the drag coefficient was carried out in rough sea conditions: wind speed and significant wave height respectively reaching  $18 \text{ ms}^{-1}$  and 6 m.

## RÉSUMÉ

Le présent article montre qu'il est possible de mesurer les flux de turbulence air-mer à partir d'une bouée en forme de disque. On y propose une méthode permettant de corriger le flux de vent mesuré dans le cas de vitesses induites par des mouvements angulaires et axiaux de l'anémomètre, ce qui permet d'évaluer le momentum, les flux de chaleur sensible et de chaleur latente. Un sous-ensemble de données recueillies pendant l'expérience sur le terrain de l'évolution des vagues (SWADE) est utilisé afin de vérifier la méthode. On a réussi à évaluer le coefficient de résistance dans le cas d'une mer démontée: la vitesse du vent et la hauteur considérable des vagues atteignant respectivement des valeurs de  $18\text{ms}^{-1}$  et de 6 m.

## 1. Introduction

This paper describes a method for the direct calculation of turbulent atmospheric fluxes of momentum, sensible heat and latent heat from a discus buoy. A buoy is the most common air-sea interaction platform around the world, allowing unattended measurements at the sea surface. Measurements of fluxes from such a platform could therefore lead to a much broader data base and thus to a better understanding of the air-sea interaction mechanisms.

The so-called "eddy correlation" method is the most direct method to determine the surface fluxes of momentum and heat, but it requires measurements, over a suitable interval and with sufficient frequency response, of two components of the air velocity, its temperature and humidity. Such measurements are usually limited to fixed platforms because of the difficulty of correcting the anemometer's measurements when it is not fixed. However, air velocity measurements from the buoy may be corrected knowing the motion of the anemometer: three rotation angles and the three components of the acceleration vector.

The proposed method is tested with data gathered for the Surface Wave Dynamics Experiment (SWADE), for which the effect of waves on air-sea coupling mechanisms is one of the primary concerns. This objective is to be achieved through an experimental plan using moored buoys, aircraft and ships (Weller *et al.* 1991). The task of continuously monitoring the waves and the surface fluxes rests mainly on the NDBC/SWADE 3 meter discus wave directional buoys (Figure 1). To the authors' knowledge, this is the first reported attempt to obtain direct estimates of the air-sea fluxes from measurements made on a small surface following buoy. The original purpose of the buoys is to observe the directional characteristics of the waves. Thus, successful flux measurements on such platforms may be examined for wave effects on the air-sea transfer coefficients.

The paper is divided as follows. Section 2 presents the experimental site, the calibration of the instruments and the environmental conditions. The proposed method to correct the air velocity measurements using the buoy's motion is presented in section 3. Results are described in section 4, and conclusions are drawn in section 5.

## 2. Description of experiment

The NDBC/SWADE 3 meter discus directional buoy instrumentation list is as follows: a directional wave measurement device (that outputs vertical acceleration, pitch and roll), Datawell's Hippy 40; a tri-axial fluxgate magnetometer, General Oceanics's 6011TAMS; three orthogonally mounted accelerometers, two Sunstrand's KA1100 and a KA1400; and a twin propeller anemometer, Young's K-Gill 35351. The major difference from the NDBC buoy standard structural configuration is the addition of a 2 m<sup>2</sup> wind vane to one of the mast legs, so that the buoy orients itself according to the wind, thereby essentially eliminating the difficulty of proper exposure of meteorological instruments. All the main buoy instruments are continuously sampled at 1 Hz by a LOPACS computer and the outputs are stored on an onboard optical disk recording system. The buoy is also intended to measure fluctuations of air temperature and specific humidity, but those instruments were not operational for the subset of the data available at this time. The anemometer height is 5 m.

All instruments were calibrated prior to mooring. The Hippy 40 was tested at the National Data Buoy Center; the magnetometer was calibrated at the Geological Survey of Canada; and the accelerometers and the anemometer were calibrated at the Canada Centre for Inland Waters (CCIW). The coordinate system was established according to the right hand rule (Figure 1), with the  $Ox_1$  axis pointing toward the buoy's bow, the  $Ox_2$  axis toward port



and the  $Ox_3$  axis upward; pitch ( $\theta$ ) is positive with the bow down, roll ( $\phi$ ) is positive with starboard down and yaw ( $\psi$ ) is positive counter-clockwise viewed from above.

The K-Gill anemometer consists of two propellers mounted at 45 deg on each side of the horizontal axis to allow updraft and downdraft winds to be measured with equal sensitivity. The horizontal and vertical wind velocities are estimated iteratively from the top and bottom propeller measurements (Ataktürk and Katsaros 1989). Particular attention has been given to the calibration of the anemometer because it has been shown (Gill 1975) that the propeller response to non-axial winds deviates from a simple cosine law. For the calibration, the K-Gill was fixed to the carriage above the 100 m towing tank at CCIW. The mounting device allowed tilt angles varying from -20 to 20 deg, while the mid-point of the line between the centers of the hubs of the propellers was kept at the same position relative to the carriage. Tests were carried out at fixed speeds (1, 2, 3, 4, 5 and 6  $\text{ms}^{-1}$ ) while the angle was altered in 5 deg steps between runs. Finally, in line calibrations were performed by rotating the K-Gill  $\pm 45$  deg from its normal vertical position.

Figure 2 shows the ratio of the measured response to the cosine law against the propeller's off-wind angle. Only the velocities ranging between 3 and 6  $\text{ms}^{-1}$  are used because the propellers are not as reliable for low wind speeds. The calibrated response ratio is described by the solid line, while  $\square$  and  $\circ$  are used for the top and bottom propellers respectively. It was found from the calibration data that the moving platform, to which the K-Gill was fixed, produced a slightly upward flow, estimated to be equivalent to a -4.8 deg tilt of the anemometer. The ratio between the measured response and the cosine law is 0.83, when the K-Gill propellers are at 45 deg to the wind. A post-experiment calibration has confirmed the above results.

### 2.1. Environmental conditions

The data set used here is a small subset of the overall SWADE experiment. It consists of 40 continuous 6-hour runs, from Discus-North (location: 38°22'05"N and 73°39'05"W, depth: 115 m), which cover three consecutive strong wind events. Figure 3 presents the wind and sea conditions that prevailed at Discus-North for the 10 day period which spans from October 17<sup>th</sup> 1990 to October 27<sup>th</sup> 1990. More specifically, there were two events with mean horizontal wind speed ( $U$ ) reaching about 15 ms<sup>-1</sup> and with significant wave height ( $H_s$ ) of 4 m, and one event with wind speed up to 18 ms<sup>-1</sup> and wave height of 6 m. Wave peak periods are also shown, they vary between 4 and 12 s. Two points near the beginning of the record show longer periods and are swell.

The mean horizontal wind speeds plotted in Figure 3 are estimated from K-Gill measurements and are corrected to compensate for the influence of angular and axial movements of the anemometer — the correction procedure will be described later. At low wind speeds the buoy will tend to align itself with the current rather than the wind. In these cases the anemometer may be facing downwind and would therefore yield negative values for the mean horizontal wind speed. Examples of this are seen in Figure 3. In cases of low wind and large swell, the angle of attack variations of the relative wind to the K-Gill may exceed  $\pm 30$  deg. In such cases the calculation of velocity components will be unreliable.

### 3. Calculation of earth referenced wind components

Eddy correlation is the only technique leading to the direct estimation of the surface fluxes. It requires that the covariance be performed between the fluctuating vertical velocity and the horizontal velocity (for the momentum flux), the air temperature (for the sensible heat

flux), and the specific humidity (for the latent heat flux). Simple direct measurements of turbulent fluxes are limited to fixed platforms. However, it is possible to measure and correct for platform motion and its effect on measured air velocity. Successful attempts to correct measurements from mobile instruments have been performed for airplanes (*e.g.* Miyake et al. 1970a) and for ships (*e.g.* Mitsuta and Fujitani 1974). In each case, the measurements of the motion of the anemometer (or its platform) allowed the correction. The same type of correction is applied here for a 3 meter discus buoy.

The K-Gill anemometer allows the determination of orthogonal wind components along the K-Gill axes ( $u_{h0}$  and  $u_{v0}$ ). The subscript h and v refer to horizontal and vertical. When "0" is appended to the subscript this refers to axes fixed in the buoy —  $v0$  is along the  $x_3$  axis (*i.e.* roughly vertical) and  $h0$  is along the  $x_1$  axis (*i.e.* roughly horizontal). In the approach we take here, the first step is to compensate for angular velocities induced by the buoy's rotations ( $V_{h0}$  and  $V_{v0}$ ), since the anemometer is not located at the center of rotation of the buoy — the rotation velocity is estimated from the derivative of the tilt angles. The second step is to compensate for the buoy's axial velocities, estimated by the integration of the accelerometer measurements ( $a_i$ ), suitable corrections having been made for the instantaneous orientation of the strapped down accelerometers package ( $a_{h0}$  and  $a_{v0}$ ). And the last step is to rotate the velocities from the K-Gill moving coordinate system to the earth coordinate system, knowing the buoy's pitch and roll angles ( $\theta$  and  $\phi$ ). Note that, for this particular experiment, the K-Gill is aligned with the buoy's bow ( $x_1$  axis). The proposed approach can be summarized as:

$$u_h = (u_{v0} \sin \theta + u_{h0} \cos \theta) + (V_{v0} \sin \theta + V_{h0} \cos \theta) + \int_{t_0}^t [a_{v0} \sin \theta + a_{h0} \cos \theta] dt$$

(1)

and

$$u_v = (u_{v0} \cos \theta - u_{h0} \sin \theta) + (V_{v0} \cos \theta - V_{h0} \sin \theta) + \int_{t_0}^t [a_{v0} \cos \theta - a_{h0} \sin \theta] dt ,$$

(2)

where

$$V_{h0} = L \frac{\partial \theta}{\partial t} \cos \alpha ,$$

$$V_{v0} = -L \frac{\partial \theta}{\partial t} \sin \alpha ,$$

$$a_{h0} = a_1 + g \sin \theta ,$$

and

$$a_{v0} = a_3 - g \cos \theta \cos \phi ,$$

for which  $u_h$  and  $u_v$  are the corrected horizontal and vertical velocities,  $L$  (5 m) is the distance between the buoy's center of gravity and the mid-point of the bisector of the line joining both propellers,  $\alpha$  (3 deg) is the angle of the line  $L$  with the buoy's vertical axis, and  $g$  ( $9.81 \text{ ms}^{-2}$ ) is the gravitational acceleration.

Since surface fluxes are influenced by even small imperfections in the levelling of the instruments, an after the fact levelling of the coordinate system is recommended (Donelan 1990). This can be achieved via the assumption that the mean vertical wind component must

vanish over a suitable averaging period. Finally, the corrected horizontal velocities are decomposed in two orthogonal components, using the horizontal orientation (yaw angle) of the buoy. It should be noted that there is no information on relative crosswind ( $x_2$  axis) velocities, so that the computation of crosswind fluctuations includes only the low frequency components to which the buoy responds.

#### 4. Computed surface fluxes

A typical run is selected to present all the intermediate results leading to the momentum flux calculations, parametrized as the drag coefficient. It is a 2048 second block (roughly 34 minutes) that starts October 19, 0000 GMT, near the peak of the first strong wind event (see Figure 3). The mean wind speed was  $12.1 \text{ ms}^{-1}$ , the significant wave height was 2.4 m, and the peak period was 7.0 s.

Figures 4 and 5 present the first 300 s of the time series that lead to the corrected horizontal and vertical air velocities. Besides the corrected air velocity, rotated from the K-Gill coordinate system to the earth reference system, these figures also show the measured air velocity, and the velocities induced by the anemometer's rotations and by the anemometer's axial movements. The corrected air velocity is the result of the addition from the measured air velocity of the velocities induced by the buoy's motions. It can be seen from Figure 4 that the measured horizontal air velocity is not dramatically altered by the angular or axial velocity contributions; however, for much lower wind speed, the buoy's motion influences the measurements enough to cause the propeller to halt or to rotate in reverse. On the other hand, the measured vertical air velocity (Figure 5) is greatly affected by the axial velocity contribution induced by the buoy's motions, while the anemometer's angular velocity influence on the vertical air velocity is negligible. Figure 6 clearly illustrates the difference

between the measured and corrected vertical air velocities. The spectral presentation, following the normalization proposed by Miyake *et al.* (1970b), shows that the signals differ in the wave energy part, and that the axial movement (heave) of the buoy is the principal cause of it. The corresponding wave surface displacement spectrum is presented in Figure 7, for which the abscissa is normalized as in Figure 6 to illustrate the direct relation between the wave field and the measured vertical velocity.

Miyake *et al.* (1970b) showed that the use of "natural coordinates", to display the air velocity spectra and cospectra, leads to universal spectral shapes for atmospheric turbulence over water *i.e.* that all such spectra should collapse one over the other (see also Busch 1973). The universal curves used in this paper have been obtained by fitting smooth shapes to the data of Miyake *et al.* (1970b). It can be seen from Figures 8 and 9 that the spectra and cospectrum, estimated from the corrected air velocities, follow those universal curves. The universal curves demonstrate that we have been able to measure the spectrum of the velocity components up to  $fz/U = 0.16$ . This is not quite up to the peak of the vertical velocity spectrum but it includes most of the cospectrum of the momentum flux (Figure 9). In fact, the measured cospectrum changes sign at higher frequencies. This change in sign is common to all cases and appears to be due to a difference in noise level at higher frequencies between the two propellers. Figure 10 shows the cospectrum plotted on log-linear axes to reveal the sign change. Only the points shown with a circle are retained. A cut-off period ( $T_{\text{cut-off}}$ ) is defined by the reciprocal of the frequency of the highest positive cospectral estimate. Beyond this point we use the universal cospectral curve to estimate and correct for the increment at high frequencies that we are unable to measure. On average, this adjustment increases our estimate of the momentum flux by about 13 %.

In order to test the procedure in the most extreme conditions experienced, it was repeated with a different 2048 second block, that starts October 26, 1850 GMT, near the peak of the third strong wind event (see Figure 3). The mean wind speed was  $14.8 \text{ ms}^{-1}$ , the significant wave height was 6.3 m, and the peak period was 12.3 s. Figures 11 and 12 show that the corrected air velocities lead to spectra and cospectra that follow the universal curves.

#### 4.1. Automatic computation

The main advantage of the use of unattended buoys to measure atmospheric fluxes is to be able to gather large data sets in a hostile environment. Consequently, an automatic computation procedure is needed — similar to that already in use by the National Data Buoy Center for wave field measurements. The proposed method to correct the measured air velocities has been applied to the 40 successive 6-hour files. Since atmospheric flux computation relies on some hypothesis, namely stability and homogeneity of the wind flow, a completely automatic procedure may lead to occasional errors and some manual post-checking is desirable, especially to avoid non-stationary atmospheric conditions. Two limitations have been identified from this analysis. First, low wind measurements may not be adequately corrected for buoy motion, if the propellers cannot precisely measure very low velocities and even reverse wind. Second, corrections must be made for the high frequency limitations of the instruments and recording system. In this demonstration analysis we dealt with the first problem by eliminating all cases in which the wind speed was below  $6 \text{ ms}^{-1}$ . The second problem was approached in the manner discussed above; that is, the cut-off period was identified. If it exceeded 3 s (the Nyquist period is 2 s), these data were rejected. Momentum flux cospectra having cut-off periods between 2 s and 3 s (graphed in Figure 13) are corrected using the universal curve. The computed drag coefficients (Figure 13) lie between 0.001 and 0.003 with occasional exceptions.

## **5. Conclusion**

This analysis has demonstrated that it is possible to measure the atmospheric surface fluxes from a discus buoy, using the eddy correlation technique. The proposed method to correct the measured wind flow, for velocities induced by angular and axial movements of the anemometer, has proven to be robust enough to handle cases with significant wave height reaching 6 m. Application limitations are the same as for measurements from a fixed platform, namely stability and homogeneity of the turbulent wind flow. Care should be taken to use a fast enough sampling frequency, to avoid losing too much of the high frequency part of the turbulent fluxes. As we have shown, the universal curves allow correction of the undersampled cospectra provided that the correction is not more than about 25%.

## **6. Acknowledgements**

This work is part of the Surface Wave Dynamics Experiment (SWADE), supported by the Office of Naval Research under contract No. N00014-88-J-1028. F.A. was supported on scholarship by the Natural Sciences and Engineering Research Council of Canada. Kimmo Kahma designed the mounting device used for calibrating the K-Gill anemometer.



## 7. References

- Ataktük, S.S. and Katsaros, K.B. 1989. The K-Gill : a twin propeller-vane anemometer for measurements of atmospheric turbulence. *Journal of Atmospheric and Oceanic Technology*, 6 (3): 509-515.
- Busch, N.E. 1973. On the mechanics of atmospheric turbulence. In *Workshop of Micrometeorology*, D.A. Haugen, Ed., American Meteorological Society, Boston, Massachusetts, 1-65.
- Donelan, M.A. 1990. Air-sea interaction. In *The Sea*, 9, B. LeMéhauté and D.M. Hanes, Eds., Wiley, New York, 239-292.
- Gill, G.C. 1975. Development and use of the UVW anemometer. *Boundary-Layer Meteorology*, 8: 475-495.
- Mitsuta, Y. and Fujitani, T. 1974. Direct measurement of turbulent fluxes on a cruising ship. *Boundary-Layer Meteorology*, 6 (1/2): 203-217.
- Miyake, M., Donelan, M. and Mitsuta, Y. 1970a. Airborne measurements of turbulent fluxes. *Journal of Geophysical Research*, 75 (24): 4506-4518.
- Miyake, M., Stewart, R.W. and Burling, R.W. 1970b. Spectra and cospectra of turbulence over water. *Quarterly Journal of the Royal Meteorological Society*, 96 (407): 138-143.
- Weller, R.A., Donelan, M.A. Briscoe, M.G. and Huang, N.E. 1991. Riding the crest: a tale of two wave experiments. *Bulletin American Meteorological Society*, 72 (2): 163-183.

**8. Figure captions**

- 1 NDBC/SWADE 3 meter discus wave directional buoy, showing the coordinate sign convention.
- 2 Calibrated response ratio of the K-Gill anemometer. The vertical lines give the standard deviations, while  $\square$  and  $\circ$  are used for the top and bottom propellers respectively.
- 3 34 minute average of the environmental conditions that prevailed during the experiment.
- 4 Time series of the horizontal air velocity corrected for buoy motion and the three terms used to compute it.
- 5 Time series of the vertical air velocity corrected for buoy motion and the three terms used to compute it.
- 6 Normalized spectra of the corrected vertical air velocity and of the principal terms used to compute it.
- 7 Surface displacement spectrum corresponding to Figure 6. The frequency axis is normalized following the air-sea fluxes convention.
- 8 Normalized spectra of the corrected horizontal ( $\square$ ) and vertical ( $\circ$ ) air velocity. The universal spectral curves proposed by Miyake *et al.* (1970b) are drawn in lighter lines. In this case the conditions were:  $U = 12.1 \text{ ms}^{-1}$ ,  $H_s = 2.4 \text{ m}$  and  $T = 7.0 \text{ s}$ .

- 9 Normalized cospectrum of the corrected horizontal and vertical air velocity. The universal cospectral curve proposed by Miyake *et al.* (1970b) is drawn with a lighter line. In this case the conditions were:  $U = 12.1 \text{ ms}^{-1}$ ,  $H_s = 2.4 \text{ m}$  and  $T = 7.0 \text{ s}$ . Note that horizontal wind velocity is negative in the coordinate system of Figure 1, so a positive cospectrum corresponds to downwind momentum fluxes.
- 10 Normalized cospectrum of the corrected horizontal and vertical air velocity. The symbols show the points that are retained.
- 11 Normalized spectra of the corrected horizontal ( $\square$ ) and vertical ( $\circ$ ) air velocity. The universal spectral curves proposed by Miyake *et al.* (1970b) are drawn in lighter lines. In this case the conditions were:  $U = 14.8 \text{ ms}^{-1}$ ,  $H_s = 6.3 \text{ m}$  and  $T = 12.3 \text{ s}$ .
- 12 Normalized cospectrum of the corrected horizontal and vertical air velocity. The universal cospectral curve proposed by Miyake *et al.* (1970b) is drawn in a lighter line. In this case the conditions were:  $U = 14.8 \text{ ms}^{-1}$ ,  $H_s = 6.3 \text{ m}$  and  $T = 12.3 \text{ s}$ .
- 13 Simultaneous presentation of the estimated drag coefficient, cut-off period and percentage of correction made to the drag coefficient, for mean corrected horizontal air velocity greater than  $6 \text{ ms}^{-1}$ .

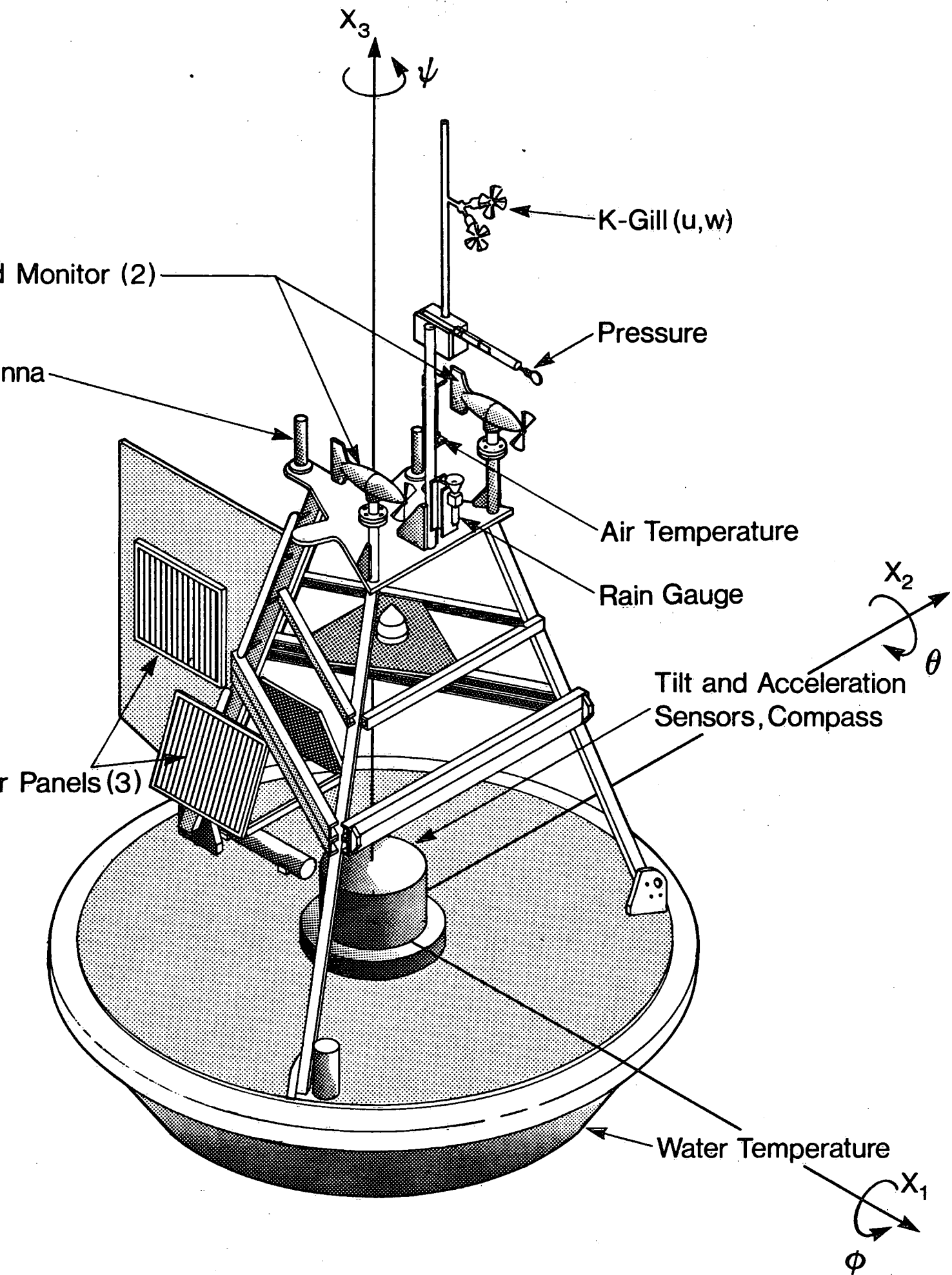


FIG. 1

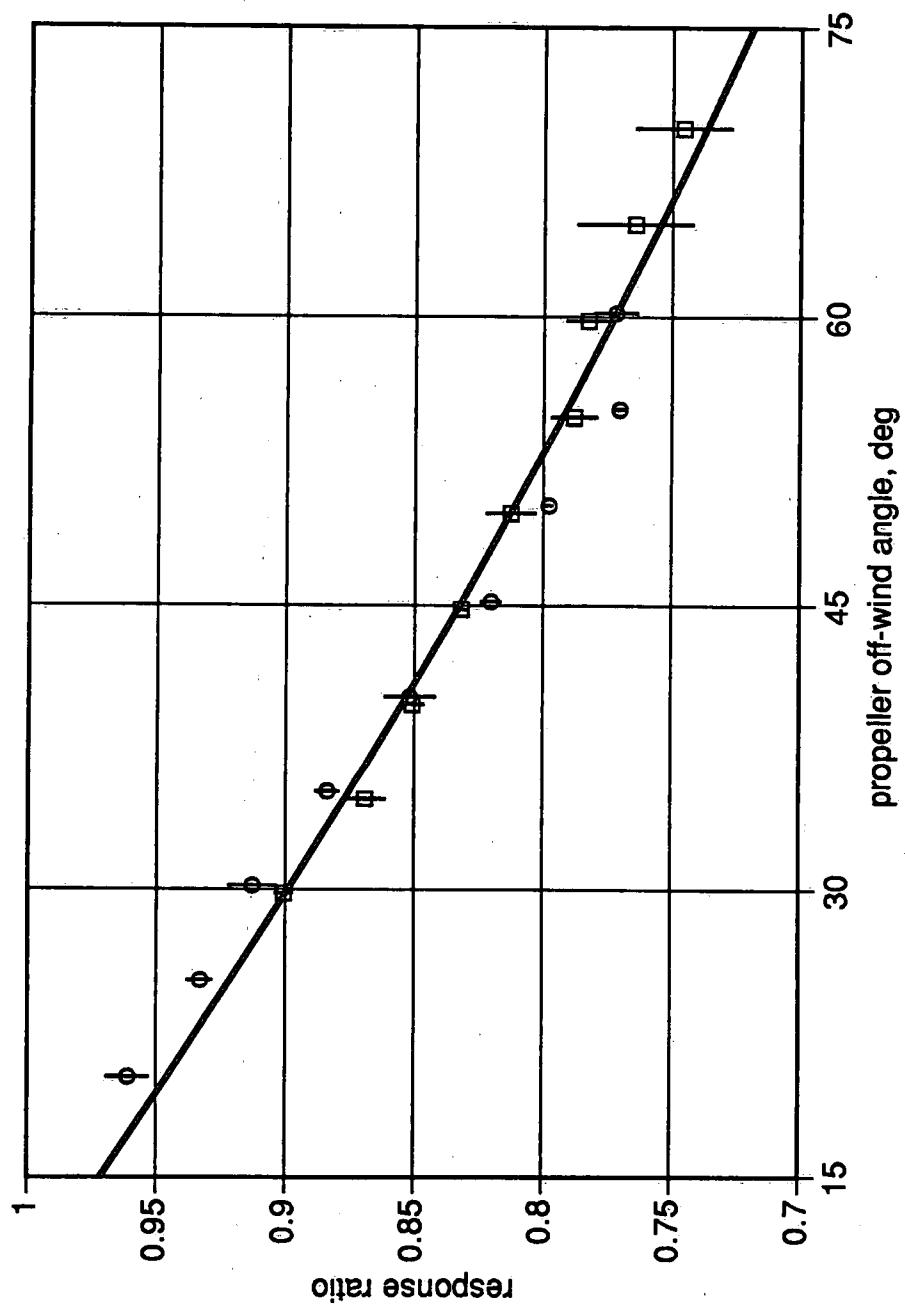


Fig. 2

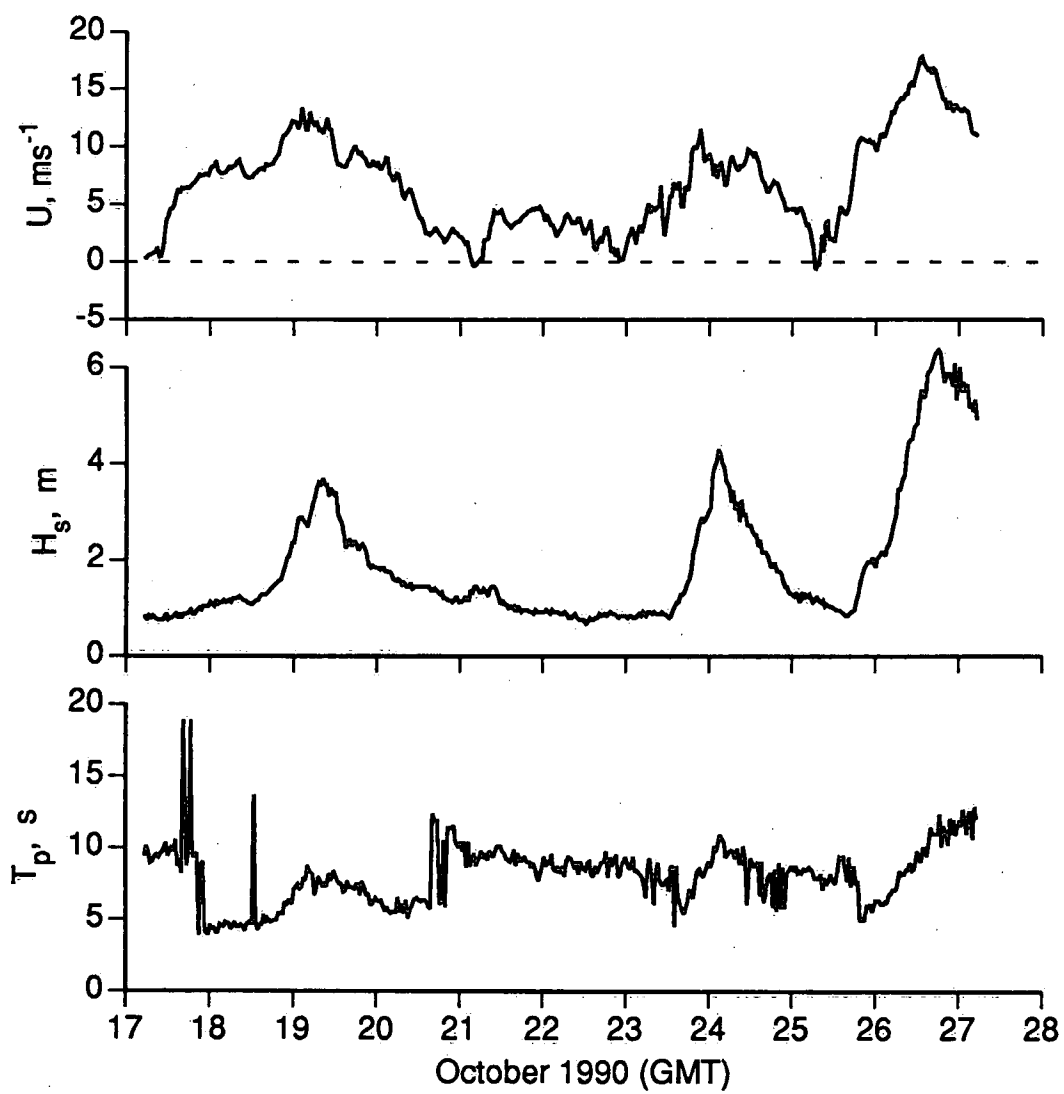


Fig. 3

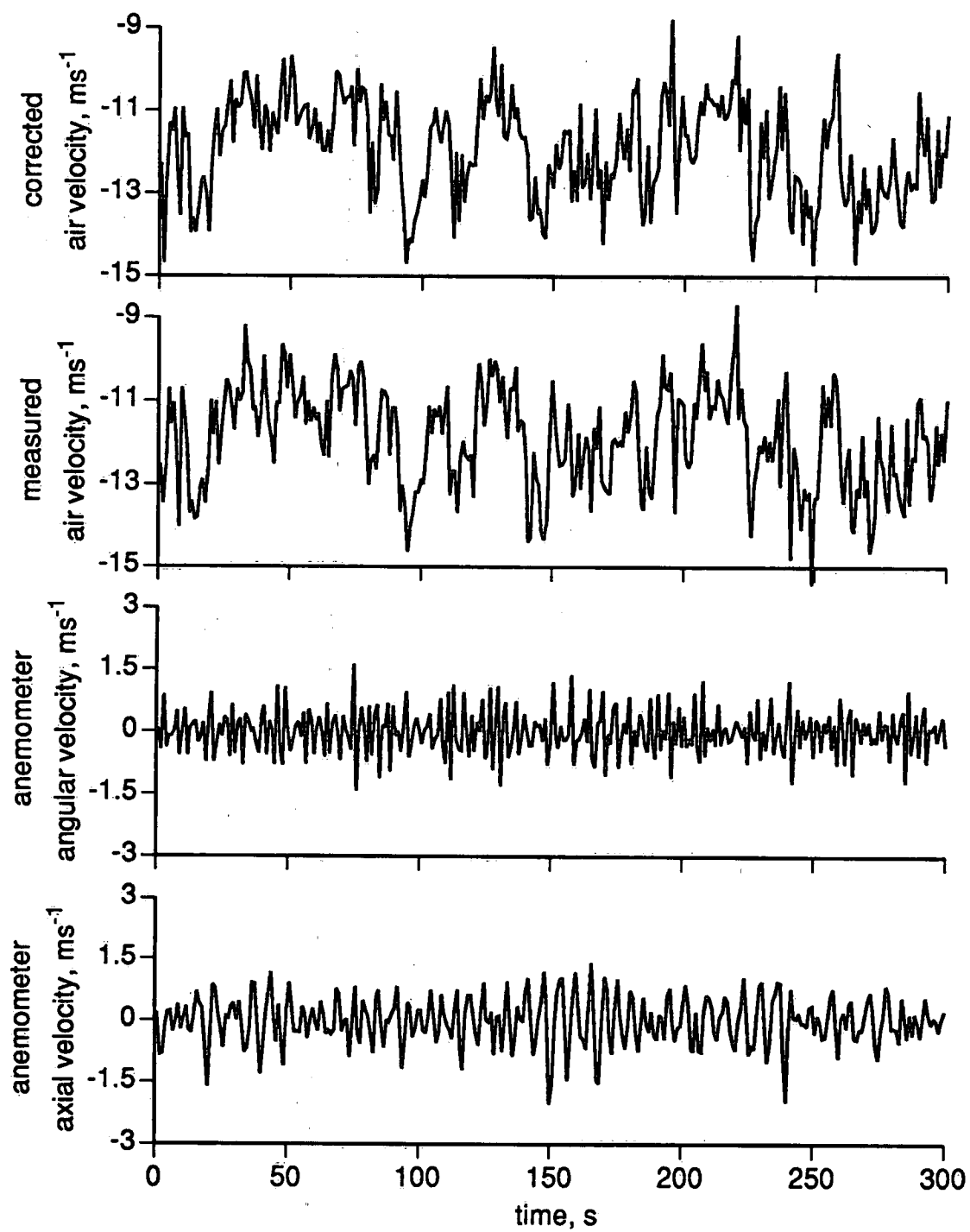


Fig. 4

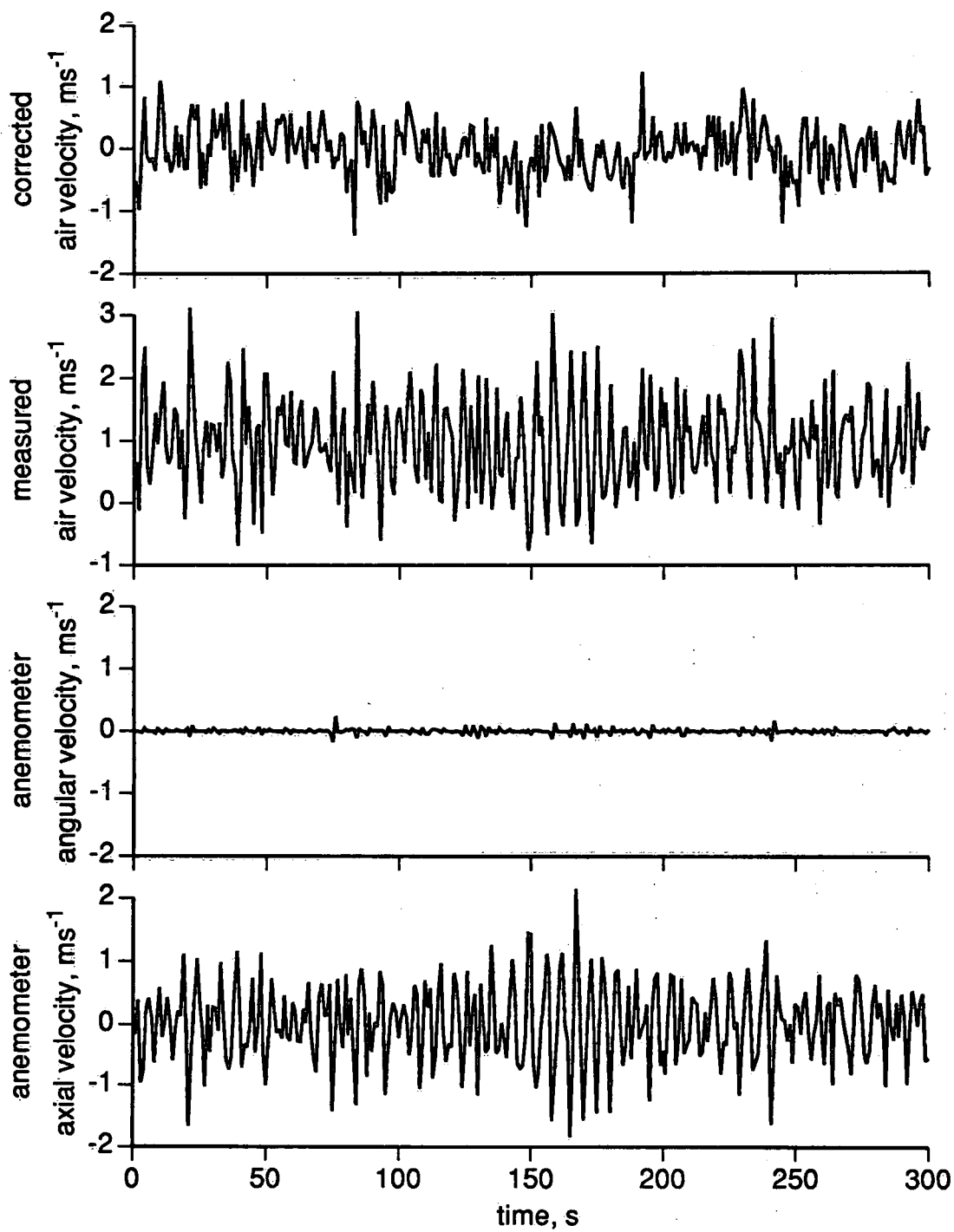


Fig. 5



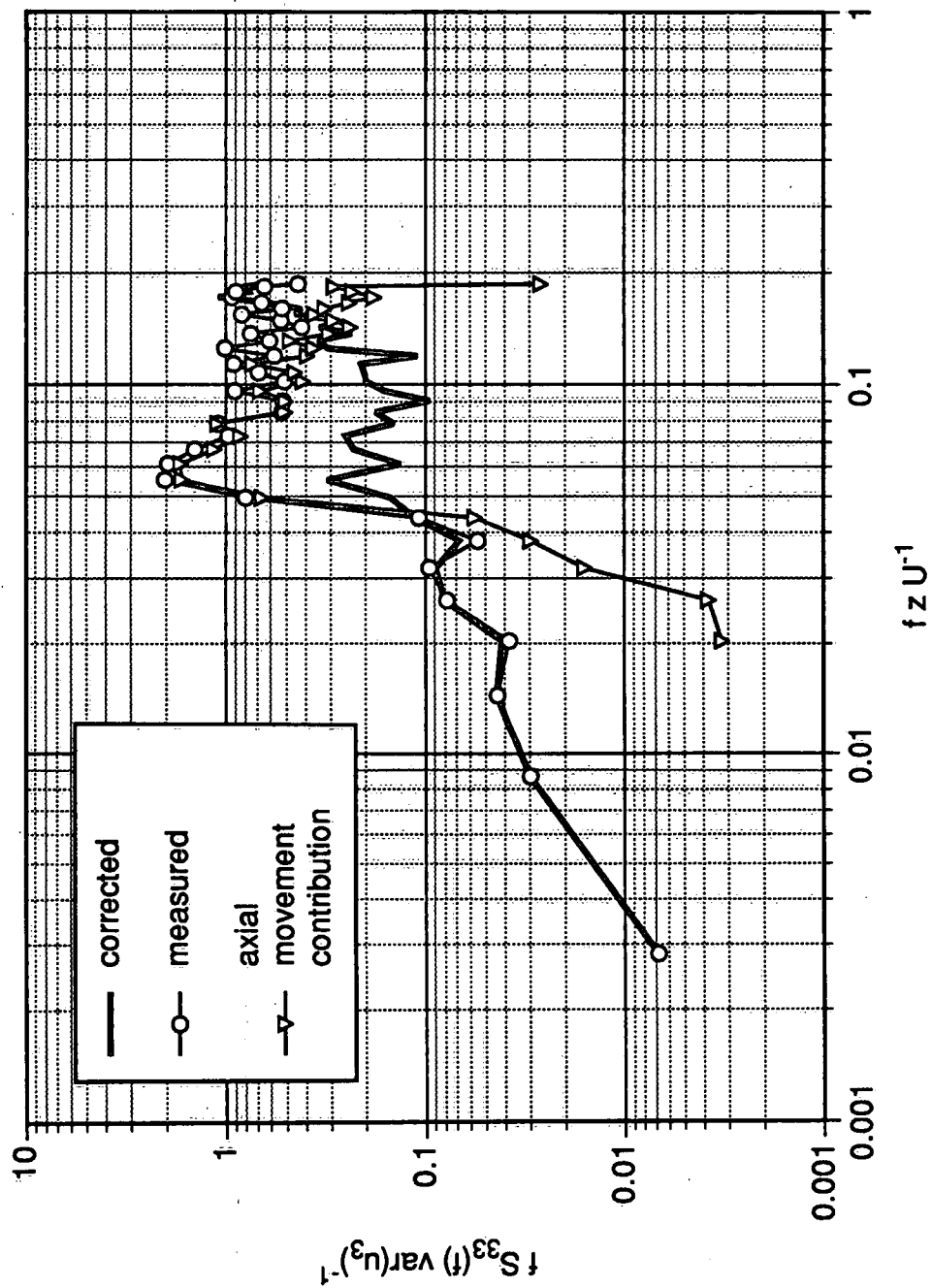


Fig. 6

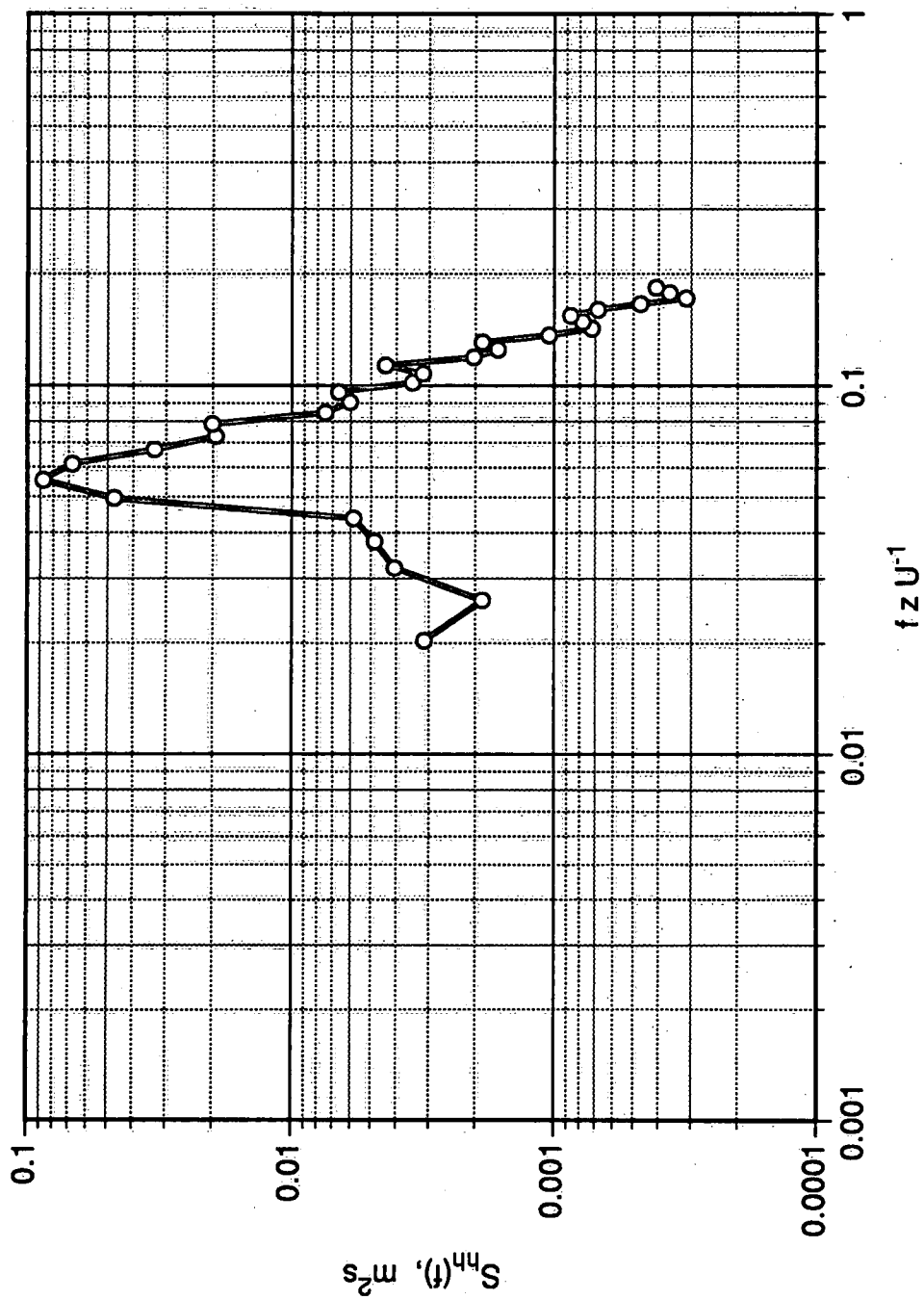


Fig. 7

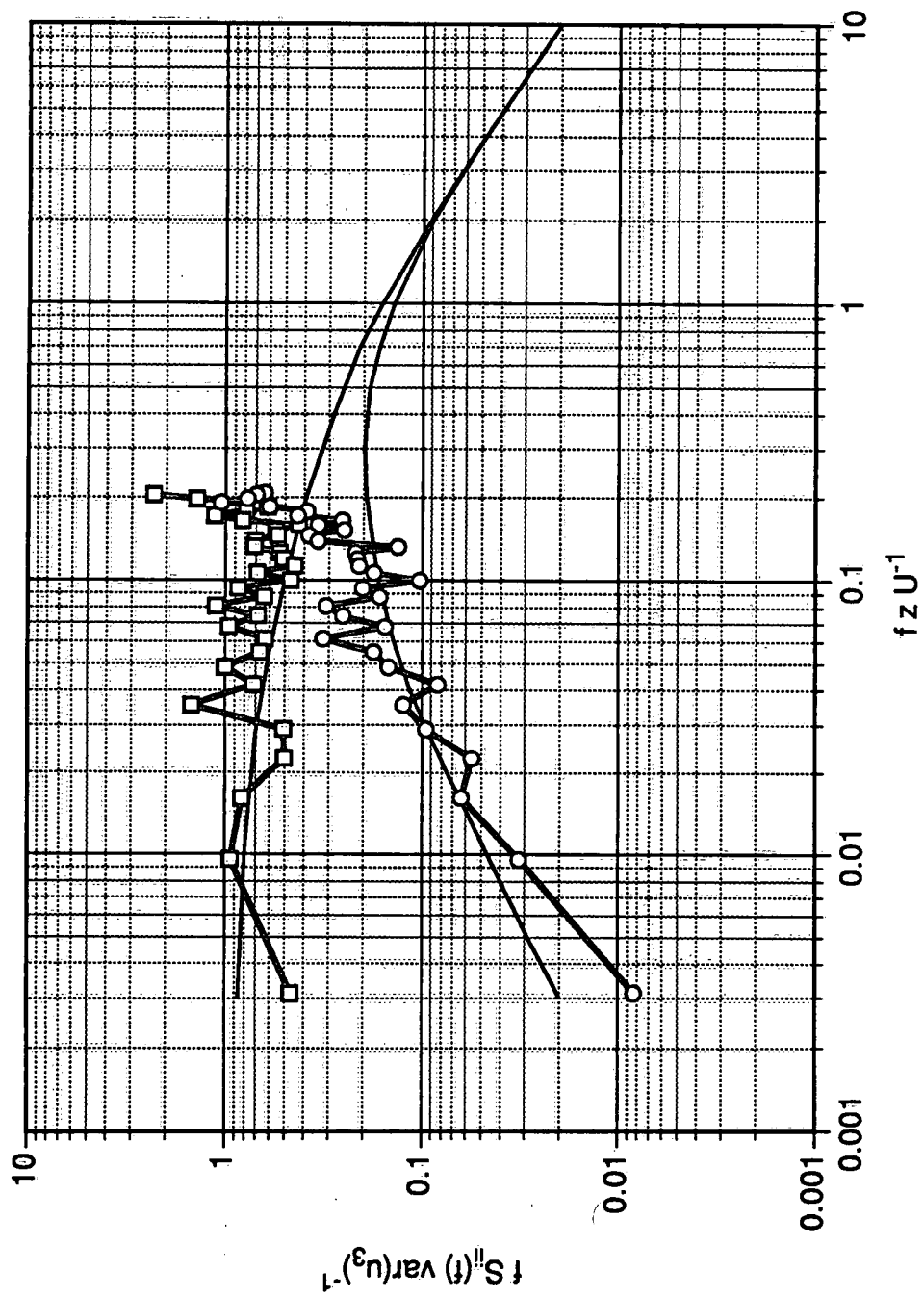


Fig. 8

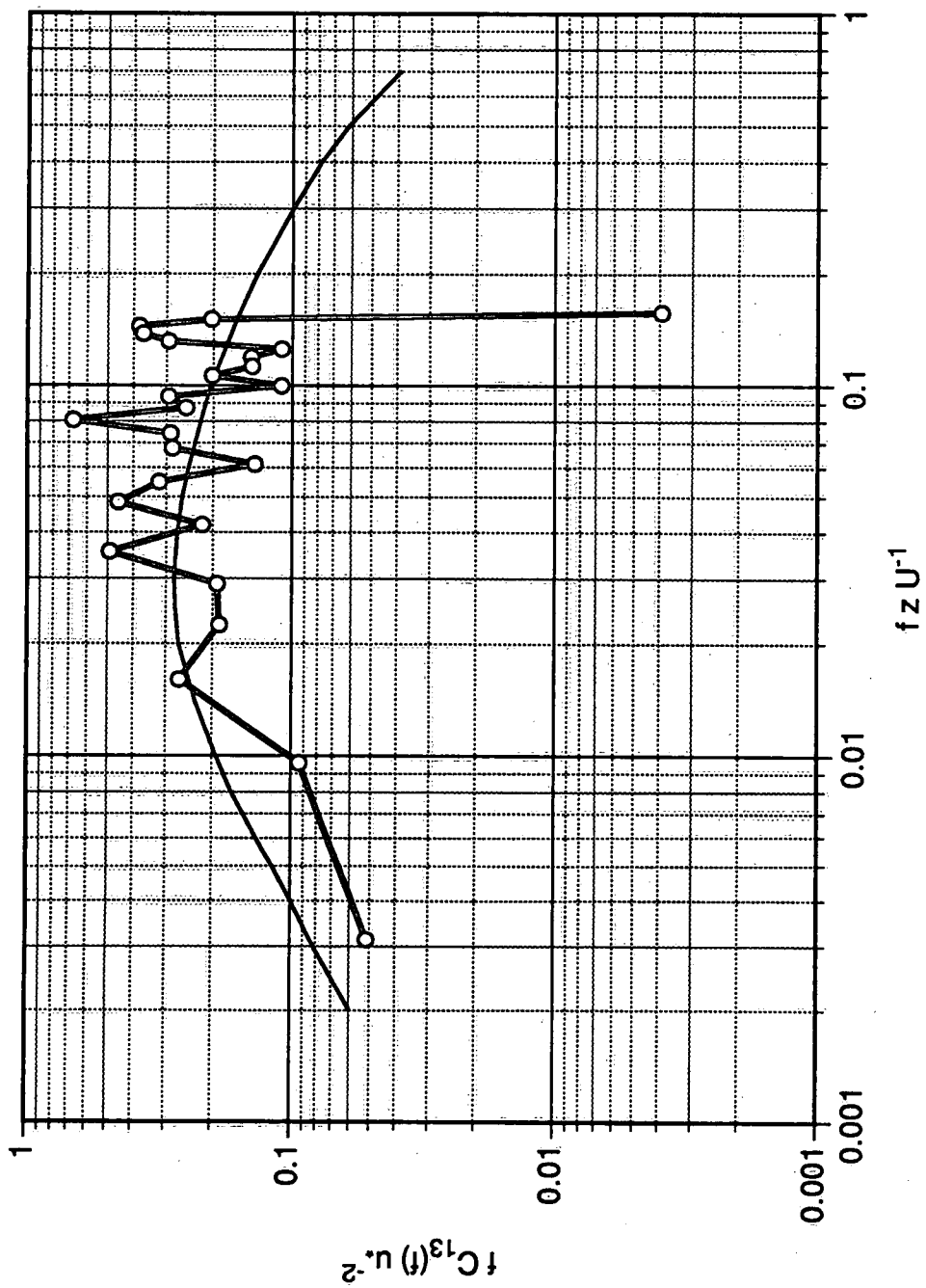


Fig. 9

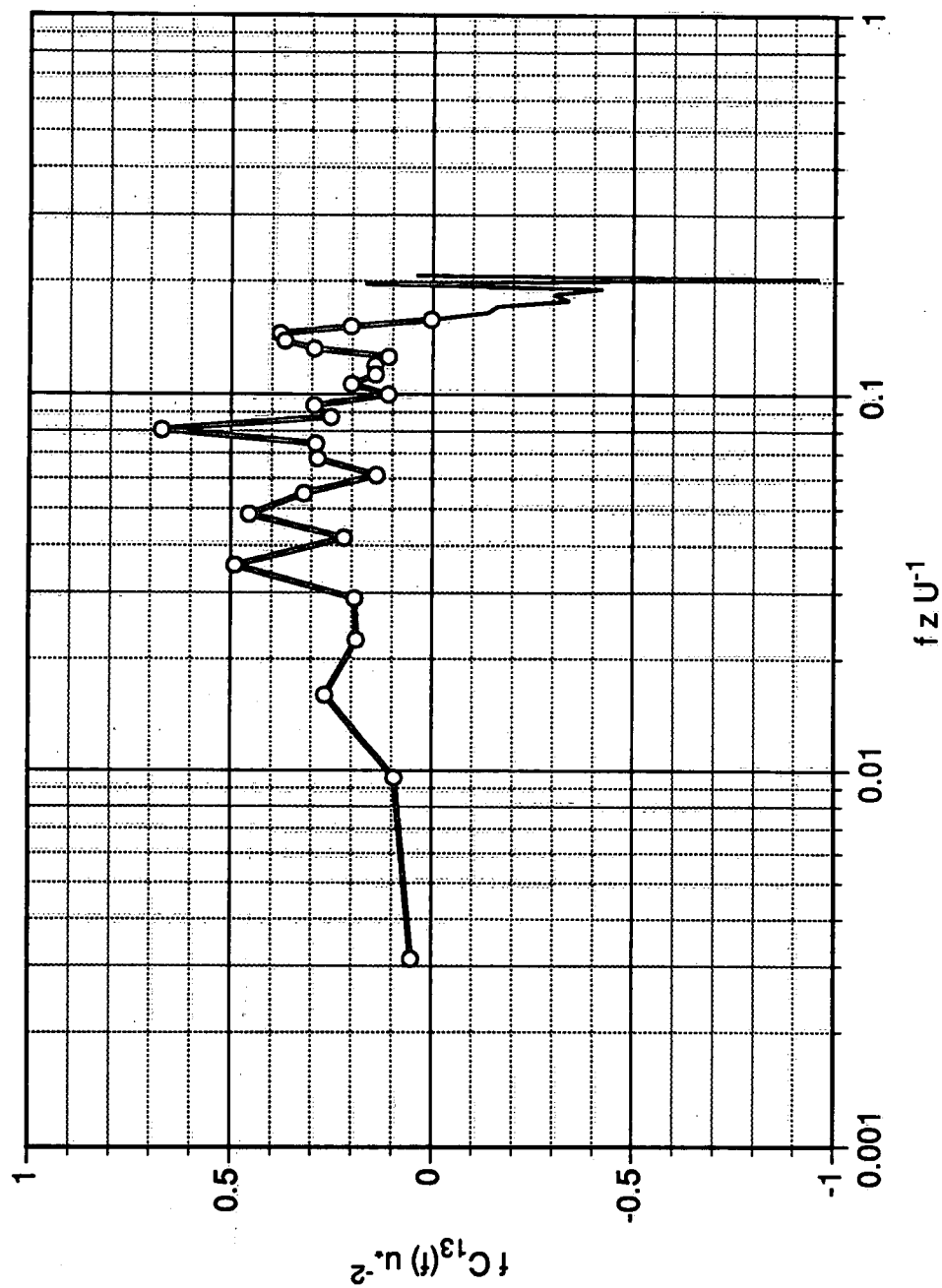


Fig. 10

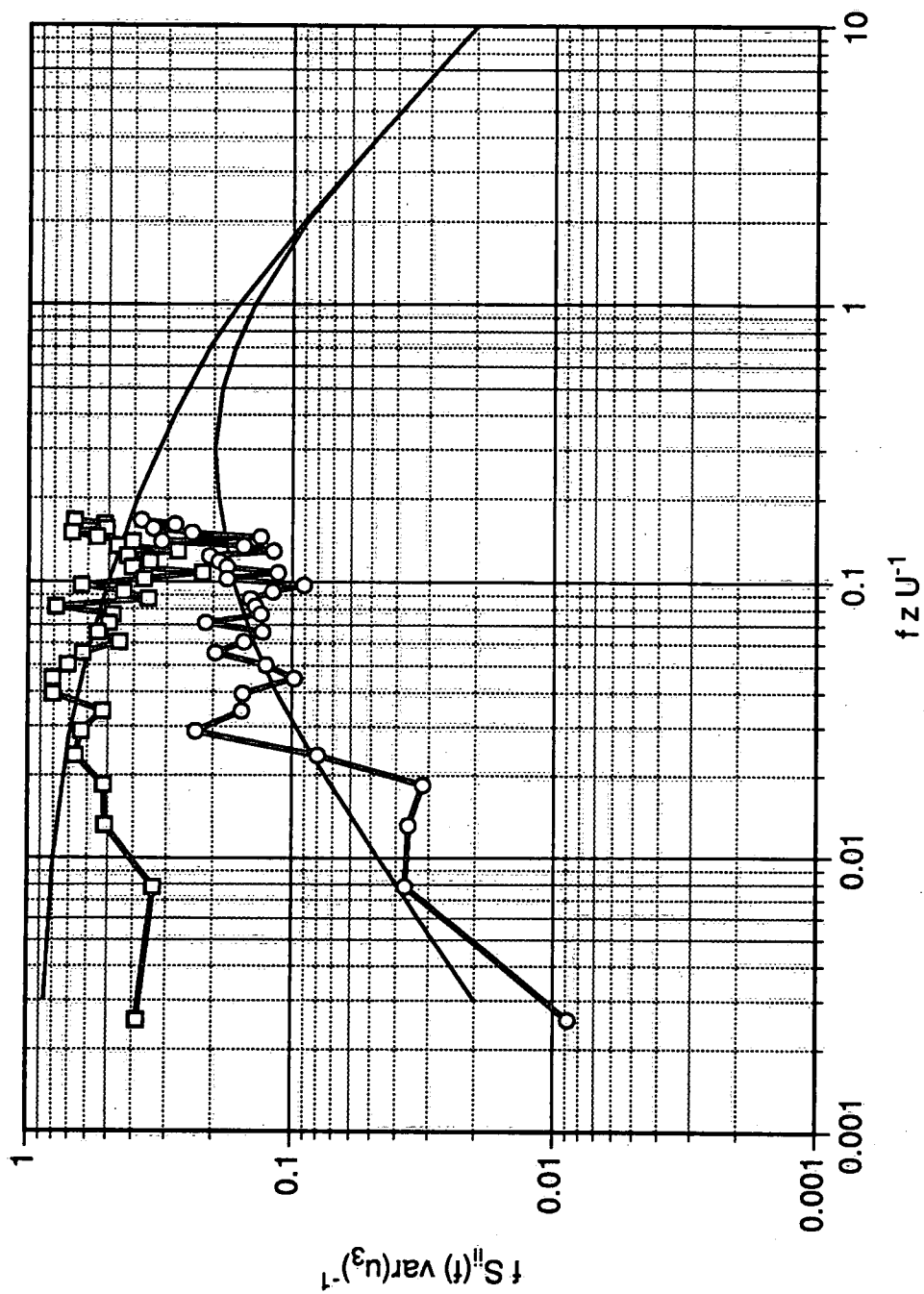


Fig. 11

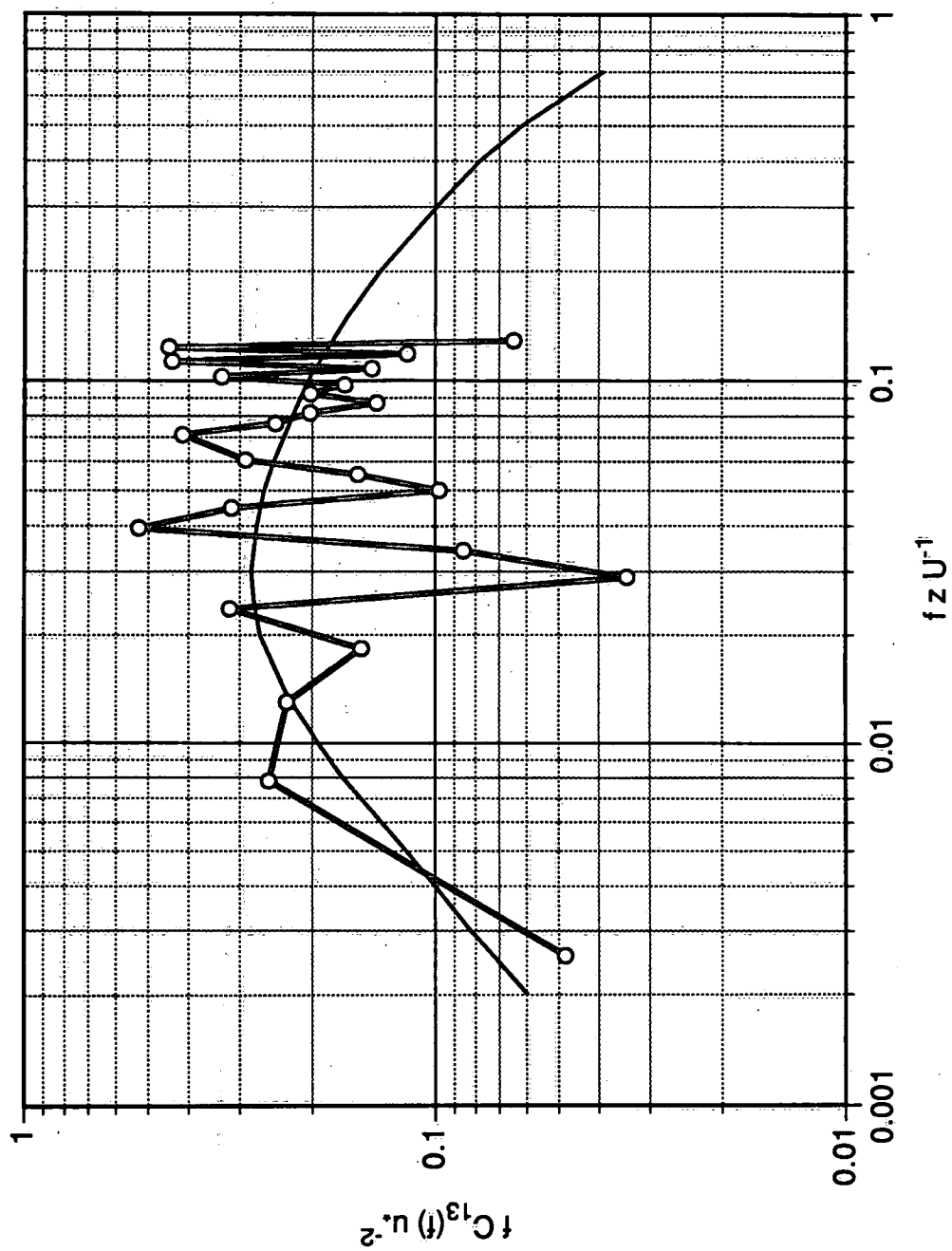


Fig. 12

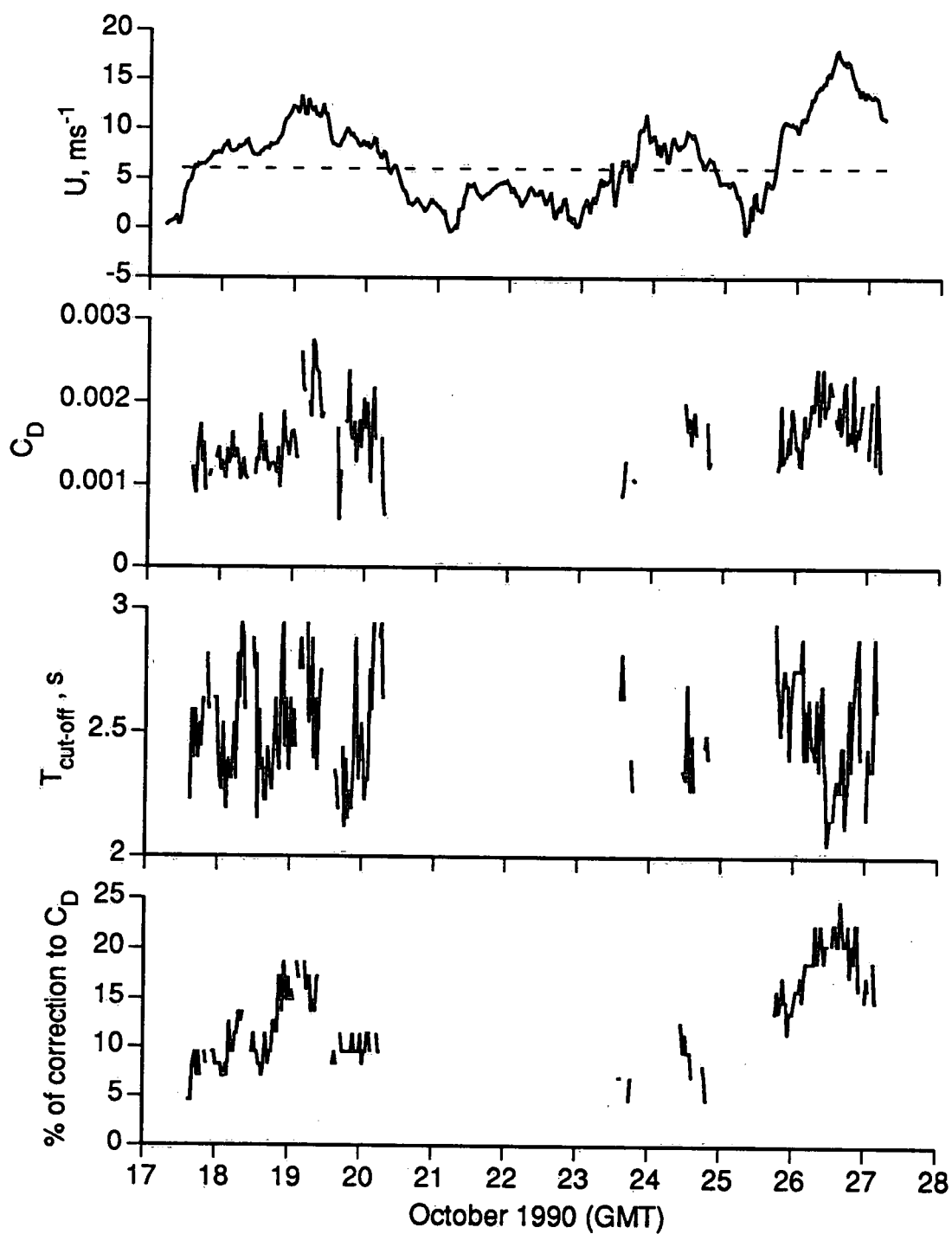
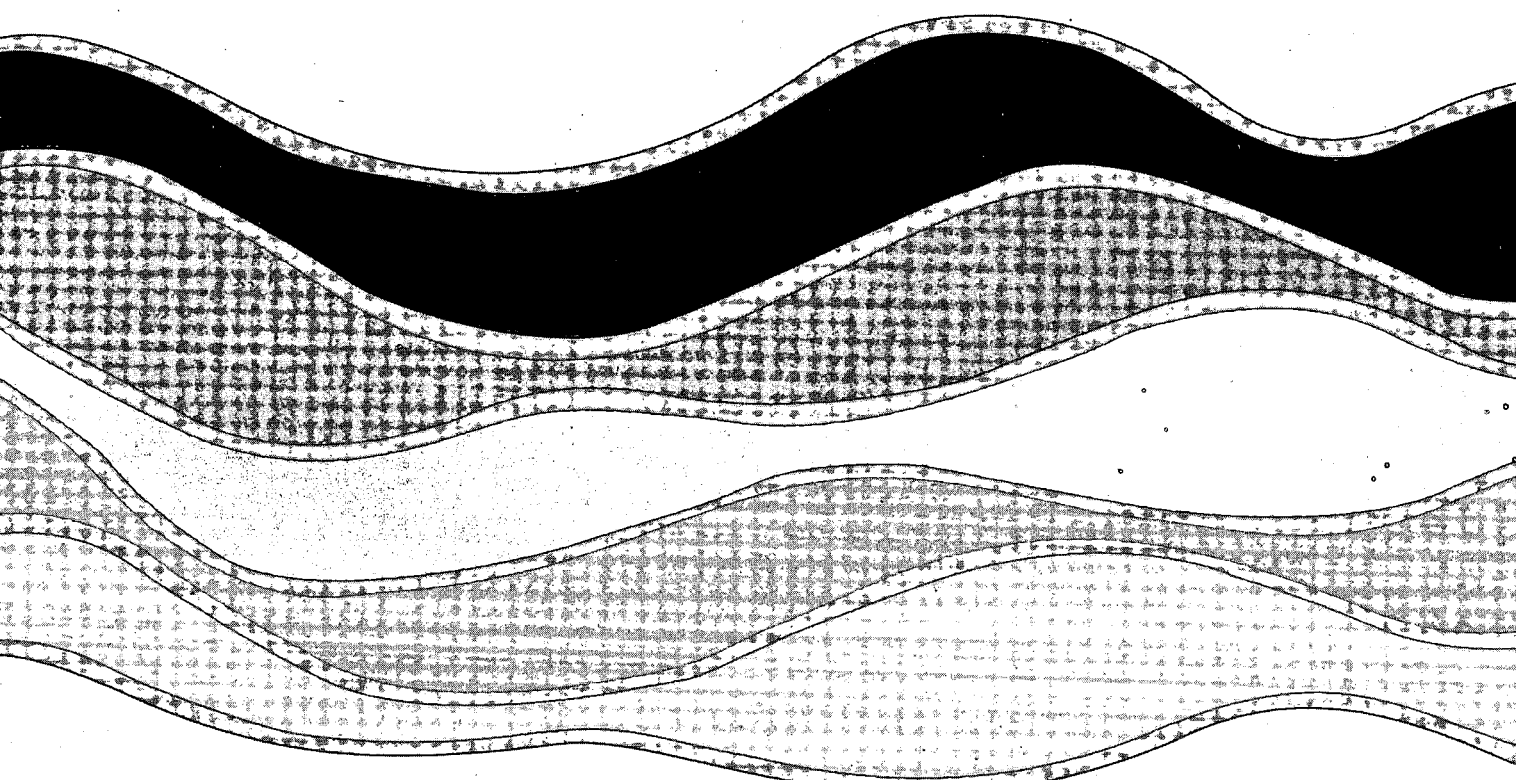


Fig. 13







NATIONAL WATER RESEARCH INSTITUTE  
P.O. BOX 5050, BURLINGTON, ONTARIO L7R 4A6

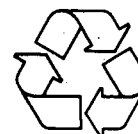


Environment Canada    Environnement Canada

Canada

INSTITUT NATIONAL DE RECHERCHE SUR LES EAUX  
C.P. 5050, BURLINGTON (ONTARIO) L7R 4A6

*Think Recycling!*



*Pensez à recycler!*